Nanochem Res 6(2): 135-142, Summer and Autumn 2021

RESEARCH PAPER

HPA-ZSM-5 nanocomposite as a highly effective and easily retrievable catalyst for the synthesis of furans

Hossein Shahbazi-Alavi[1,*], Raheleh Teymuri[2], Javad Safaei-Ghomi[2]

[1] Young Researchers and Elite Club, Kashan Branch, Islamic Azad University, Kashan, Iran.

[2] Department of Organic Chemistry, Faculty of Chemistry, University of Kashan, Kashan, Iran.

ARTICLE INFO

Article History:
Received 15 July 2021
Accepted 15 September 2021
Published 15 October 2021

Keywords:
Zeolite
HPA-ZSM
Furan
Nanocatalyst

ABSTRACT

HPA-ZSM-5 nanocomposite as a green heterogeneous catalyst was utilized for the synthesis of furans by the three-component reaction of phenylglyoxal, dimethyl acetylenedicarboxylate and primary amines. The best results were obtained in the presence of 6 mg of HPA-ZSM-5 nanocomposite in CH_2Cl_2 at room temperature. The zeolite catalyst has been characterized by X-ray diffraction (XRD), field emission scanning electron microscopes (FE-SEM), energy dispersive spectroscopy (EDS), Fourier transform infrared (FT-IR), and N_2-adsorption analysis. Experimental simplicity, wide range of products, excellent yields in short reaction times, reusability of the catalyst, and low catalyst loading are some of the substantial features of this method.

How to cite this article
Shahbazi-Alavi H., Teymuri R., Safaei-Ghomi J. HPA-ZSM-5 nanocomposite as a highly effective and easily retrievable catalyst for the synthesis of furans. Nanochem Res, 2021; 6(2):135-142. DOI: 10.22036/ncr.2021.02.001

INTRODUCTION

Furan derivatives indicate anti-oxidation [1], antimicrobial [2], antimalarial [3], anticancer [4], anti-AIDS [5], anti-inflammatory [6], and anti-diabetic [7] activities. The exploration of effective procedures for the synthesis of furans is a serious challenge. The preparation of furans has been studied using catalysts including $K[Al(SO_4)_2].12H_2O$ [8], N-methyl 2-pyrrolidonium hydrogen sulfate [9], formic acid [10], $SnCl_2.2H_2O$ [11], β-cyclodextrin [12], tetra-*n*-butylammonium bisulfate [13], $Al(HSO_4)_3$ [14], HY Zeolite [15] and Vitamin B12 [16]. Each of these catalysts may have its own benefits but also suffer apparent disadvantages such as high reaction times, complicated work-up, low efficiency, or unwanted reaction conditions. Despite the use of these procedures, there remains a need for further new ways for the preparation of furans. Nanocatalysts have obtained notable attention as effective catalysts in many organic reactions due to their high surface-to-volume ratio and coordination parts which create a larger number of active sites per unit area in comparison with their heterogeneous counter sites [17-18]. Heteropolyacids (HPAs) have polyoxometalate inorganic cages, which may adopt the Keggin structure with the common formula $H_3MX_{12}O_{40}$, where X is the heteroatom and M is the central atom. Generally M can be either Si or P, and X = Mo or W [19]. Immobilization of HPAs on silica structures as support results in more stability and increased catalytic activity [20-21]. Heteropolyacids have been heterogenized using immobilization of HPAs on zirconium dioxide [22], titanium dioxide [23], silica [24-25], zeolite [26] and SBA-15 or MCM-41 [27-28]. In this context, among different solid supports,

* Corresponding Author Email: *hosseinshahbazi99@yahoo.com*

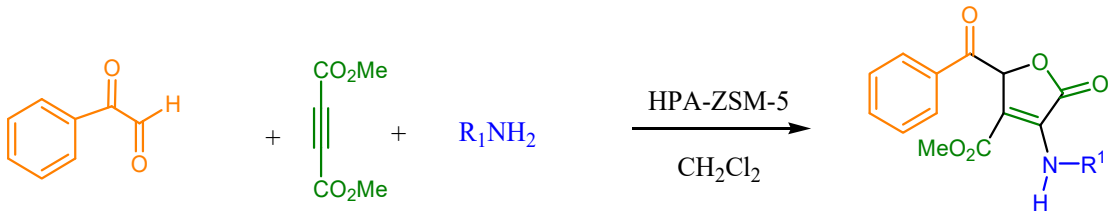

1 **2** **3** **4a-4h**

Scheme 1. Synthesis of furans

nanocrystalline ZSM-5 zeolite is most preferred owing to its many advantageous properties such as high surface area with different active sites, small pore sizes, short diffusion path, excellent chemical and thermal stability, and good accessibility [29-30]. Herein, we report the use of HPA-ZSM-5 as an efficient catalyst for the preparation of furans by the multi-component reactions of phenylglyoxal, dimethyl acetylenedicarboxylate and primary amines (Scheme 1).

EXPERIMENTAL METHOD

Chemicals and apparatus

All organic materials were purchased commercially from Sigma-Aldrich and Merck. Powder X-ray diffraction (XRD) was performed on a Philips diffractometer of X'pert Company with monochromatized Cu Kα radiation (λ = 1.5406 Å). Microscopic morphology of the nanocatalyst was visualized by SEM (MIRA3). The IR spectra were recorded on FT-IR Magna 550 apparatus using KBr plates. The energy-dispersive X-ray spectroscopy (EDS) measurement was carried out with the SAMX analyzer. The N_2 adsorption/desorption analysis (BET) was performed using an automated gas adsorption analyzer (BEL SORP mini II).

Preparation of ZSM-5

The zeolite precursor was prepared by adding tetrapropylammonium hydroxide (TPAOH) and tetraethyl orthosilicate (TEOS) to a mixed aqueous solution of aluminium isopropoxide [Al(*i*Pro)$_3$] and NaOH with stirring. The mixture was converted to a gel. The gel was stirred for 20 h. The molar composition of the gel was $1Al_2O_3$:$46SiO_2$:4TPA:$5Na_2O$:$2500H_2O$. The resulting gel was sealed in Teflon-lined autoclaves and heated at 165 °C for 72h. The solid product was recovered by filtration, washed by deionized water for several times, dried in an oven at 100 °C overnight. The as-synthesized material was then calcined at 550 °C for 8h.

Preparation of HPA-ZSM-5

ZSM-5 Zeolites (1 g) was added to the solution of 0.3 g of phosphomolybdic acid (HPA) in ethanol (25 mL) and the reaction mixture was stirred for 24h. The mixture was filtered, washed by deionized water for several times, and dried in an oven at 100 °C overnight. The as-synthesized material was subjected to product HPA-ZSM-5 at 400 °C for 2h. The calcined materials was transferred to desiccator and then converted into fine particles using a mortar and pestle.

General procedure for the preparation of furans (4a-h)

A mixture of amine (1 mmol), dimethyl acetylenedicarboxylate (1 mmol), phenylglyoxal (1 mmol) and HPA-ZSM-5 (6 mg) was stirred in dichloromethane (10 mL) at room temperature. After completion, as indicated by TLC (EtOAc-petroleum ether, 2:8), the nanocatalyst was separated from the mixture using filtration. The solvent was evaporated under vacuum and the products were obtained. The characterization data of the compounds of **4a** and **4b** are given below.

Methyl 2-benzoyl-4-[(2-methoxybenzyl)amino]-5-oxo-2,5-dihydro-3-furancarboxylate (4a)

Yellow oil, FT-IR (KBr): 3402, 3052, 3004, 1771, 1705, 1675, 1604, 1476, 1122 cm^{-1} ; ^{1}H NMR δ 8.04-6.92 (m, 9H, ArH), 6.25 (s, 1H, CH), 5.02-4.95 (m, 2H, CH_2), 3.87, 3.56 (2s, 6H, 2MeO), 2.20 (s, 1H, NH). ^{13}C NMR δ 192.4, 164.5, 164.4, 157.3, 136.4, 135.2, 129.5, 129.4, 128.4, 128.1, 127.4, 126.7, 124.3, 110.6, 105.3, 76.1, 56.9, 52.5, 42.8. Anal. Calcd. for $C_{21}H_{19}NO_6$: C 66.13, H 5.02, N 3.67. Found: C 66.16, H 4.94, N 3.721.

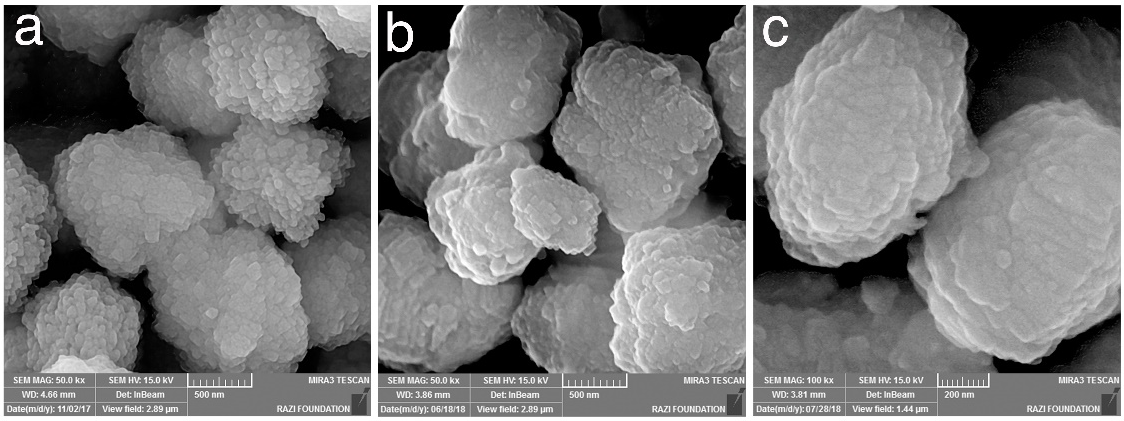

Fig. 1. FE-SEM images of (a) ZSM-5, (b) HPA-ZSM-5, (c) the used HPA-ZSM-5

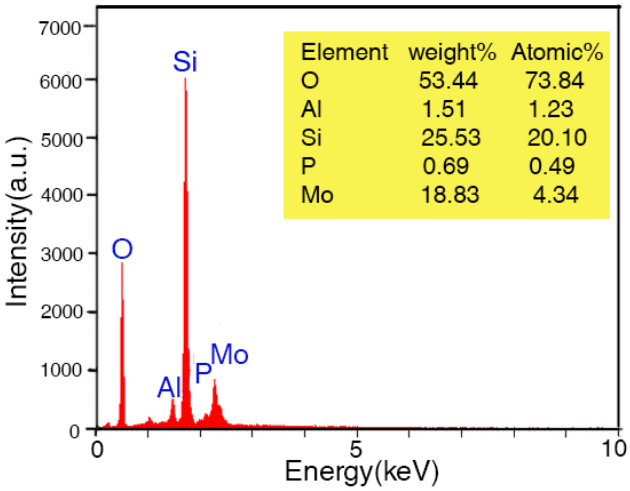

Fig. 2. EDS of HPA-ZSM-5

Methyl 2-benzoyl-4-[(4-methoxybenzyl)amino]-5-oxo-2,5-dihydro-3-furancarboxylate (4b)

Yellow oil, FT-IR (KBr): 3302, 3105, 3006, 1752, 1702, 1675, 1602, 1478, 1468, 1379, 1102 cm^{-1} ; ^{1}H NMR δ 8.09-6.92 (m, 9H, ArH), 6.42 (s, 1H, CH), 4.92-4.80 (m, 2H, CH_2), 3.84, 3.52 (2s, 6H, 2MeO), 2.69 (s, 1H, NH), ^{13}C NMR δ 192.6, 169.1, 162.4, 159.2, 156.4, 155.2, 154.1, 153.2, 135.2, 135.1, 107.2, 105.4, 76.1, 60.2, 57.4, 44.6. Anal. Calcd. for $C_{21}H_{19}NO_6$: C, 66.13; H, 5.02; N, 3.67;. Found: C, 66.15; H, 5.07; N, 3.72.

RESULTS AND DISCUSSION

The prepared catalyst was characterized by XRD, FE-SEM, EDS, FT-IR and BET analyses.

FE-SEM images of ZSM-5 and HPA-ZSM-5 are provided in Fig. 1. After the immobilization, the surfaces of the catalyst, covered with a white translucent substance, became smoother. The particles became larger in size and their profiles clearer, indicating that HPA was immobilized on the surface of ZSM-5. The evaluation of the used catalyst structure by FE-SEM provides evidence that the morphology of the catalyst remained unchanged after the 5th cycle (Fig. 1b, 1c).

EDX analysis (Fig. 2) of the catalyst demonstrated the presence of Al, P, O, Si, and Mo elements, confirming the formation of the catalytic system as visualized. Elemental mapping images of the catalyst showed uniform distribution of the elements P and Mo in the desired catalytic system.

The XRD patterns of ZSM-5 and HPA-ZSM-5 are shown in Fig. 3. In pattern (a), the peaks of high intensity at 23.4°, 24.1°, and 24.6°

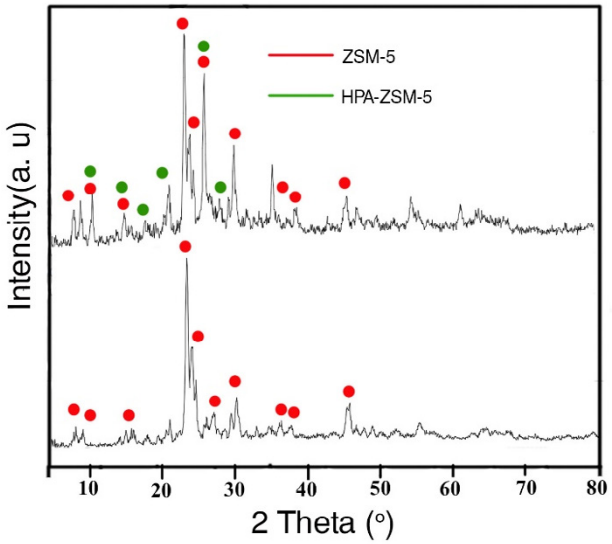

Fig. 3. XRD of ZSM-5 and HPA-ZSM-5

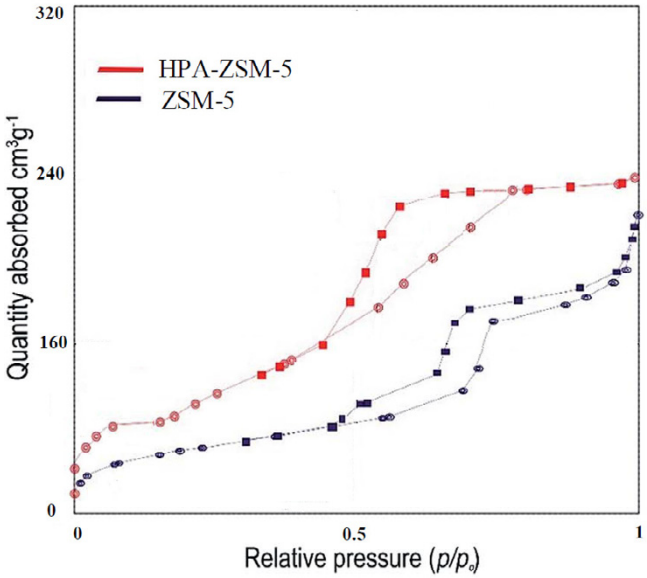

Fig. 4. N_2 adsorption–desorption isotherms of ZSM-5 and HPA-ZSM-5

are the characteristic diffraction peaks of ZSM-5, indicating good crystallinity of our synthesized ZSM-5. Compared with the ZSM-5 pattern, the HPA-ZSM-5 pattern exhibits all the diffraction peaks of ZSM-5, and the shape and intensity of the diffraction peaks have negligible changes, indicating that the prepared catalysts maintained the good crystallinity of ZSM-5 after the immobilization of the HPA onto ZSM-5. The particle size of HPA-ZSM-5 calculated by the Debye–Scherer equation is about 42 nm.

N_2-sorption isotherms at 77 K of ZSM-5 and HPA-ZSM-5 were indicated in Fig. 4. As shown in Fig. 4, all the isotherms exhibited a typical type IV isotherm with an H1 hysteresis loop starting from $P/P0$ = 0.5. The results demonstrate that the BET specific surface area of ZSM-5 increased from 170 to 240 m^2/g after modification with HPA. Nanostructures exhibit good catalytic activity due to their large surface area and active sites which are mainly responsible for their catalytic activity [31-36].

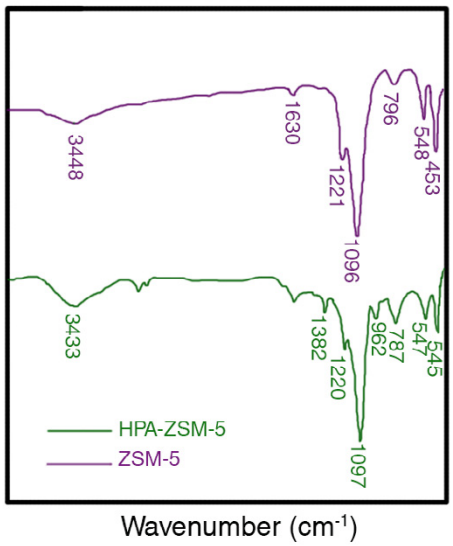

Fig. 5. Fourier-transform infrared spectroscopy spectra of ZSM-5, HPA-ZSM-5

Table 1: Optimization of reaction conditions [a]

Entry	Solvent	Catalyst (amount)	Time (min)	Yield [b] %
1	CH_2Cl_2	—	400	12
2	CH_2Cl_2	Et_3N (6 mol%)	250	39
3	CH_2Cl_2	$ZrOCl_2.8H_2O$ (6 mol%)	300	26
4	CH_2Cl_2	*p*-TSA (10 mol%)	300	15
5	CH_2Cl_2	ZSM-5 (8 mg)	300	42
6	CH_2Cl_2	HPA (5 mg)	200	62
7	CH_2Cl_2	nano-ZnO (8 mg)	200	42
8	CH_2Cl_2	HPA-ZSM-5 (4 mg)	80	85
9	CH_2Cl_2	HPA-ZSM-5 (6 mg)	80	95
10	CH_2Cl_2	HPA-ZSM-5 (8 mg)	80	95
11	CH_3CN	HPA-ZSM-5 (6 mg)	120	52
12	$CHCl_3$	HPA-ZSM-5 (6 mg)	100	84
13	DMF	HPA-ZSM-5 (6 mg)	120	62
14	EtOH	HPA-ZSM-5 (6 mg)	160	40

[a] Reaction conditions: 2-methoxybenzylamine (1 mmol) dimethyl acetylenedicarboxylate (1 mmol), phenylglyoxal (1 mmol)
[b] Isolated yield

FT-IR studies on zeolite ZSM-5 and HPA-ZSM-5 were conducted (Fig. 5). ZSM-5 has bands at the following wavenumbers (cm^{-1}): 548, 796, 1096 (absorptions of SiO_2), 1630 (adsorbed H_2O) and 3448 (O-H). The bands at 787 and 962 cm^{-1} are typical for Keggin's structure of heteropolyacids and corresponds to vasMo-O-Mo vibrations [25, 37].

At first, to find the optimum conditions, the one-pot reaction of 2-methoxybenzylamine, dimethyl acetylenedicarboxylate and phenylglyoxal in the presence of the diverse catalysts and solvents was selected as the model reaction for the preparation of 5-oxo-2,5-dihydro-3-furancarboxylates. The best results were obtained in dichloromethane and we found that the reaction provided convincing results in the presence of HPA-ZSM-5 (6 mg) at room temperature (Table 1). In this reaction, the nanocatalyst in non-polar solvents such as CH_2Cl_2 and $CHCl_3$ shows more activity. After that,

Table 2: Synthesis of 5-oxo-2,5-dihydro-3-furancarboxylates using HPA-ZSM-5 [a]

Entry	primary amine	product	Time (min)	Yield [b] %
1	2-methoxybenzylamine **3a**	**4a**	80	95
2	4-methoxybenzylamine **3b**	**4b**	80	93
3	4-methylbenzylamine **3c**	**4c**	90	89
4	benzylamine **3d**	**4d**	100	88
5	4-fluorobenzylamine **3e**	**4e**	120	85
6	propylamine **3f**	**4f**	110	82
7	(furan-2-yl)methanamine **3g**	**4g**	100	87
8	3,4-dichlorobenzylamine **3h**	**4h**	110	85

[a] Reaction conditions: primary amines (1 mmol) dimethyl acetylenedicarboxylate (1 mmol), phenylglyoxal (1 mmol)
[b] Isolated yield

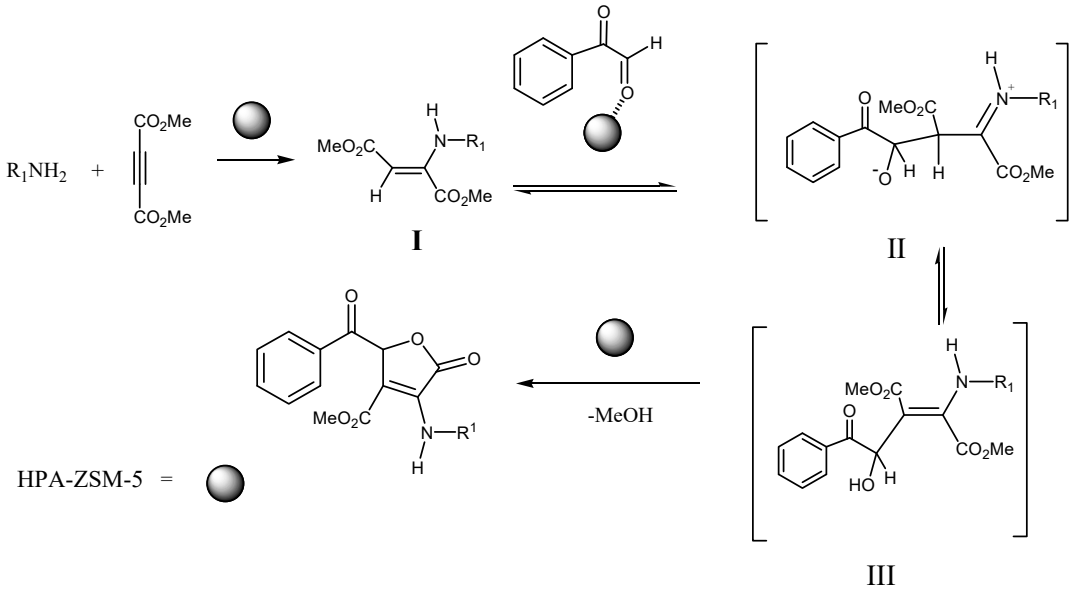

Scheme 2. Schematic mechanism for the catalytic activity of HPA-ZSM-5 for the synthesis of furans

the obtained optimal conditions were applied to perform the reaction of different primary amines in the presence of HPA-ZSM-5 (6 mg) as catalyst, in order to afford the corresponding products in high to excellent yields (Table 2).

The reusability of the nanocatalyst was studied for the model reaction, and it was found that the product yields lessened only to a very small extent on each reuse (run 1, 95%; run 2, 95%; run 3, 94%; run 4, 94%; run 5, 93%, run 6, 93%). After the completion of the reaction (as determined by TLC), since HPA-ZSM-5 was insoluble in CH_2Cl_2, it could be obtained by simple filtration. The catalyst was washed four times with ethanol and dried at room temperature for 15h prior to re-use.

Scheme 2 shows a plausible mechanism for this

reaction in the presence of HPA-ZSM-5. At first, the nucleophilic attack by the amine on dimethyl acetylenedicarboxylate generates aminobutendioate **I** as an electron-rich enaminone. The subsequent nucleophilic attack of aminobutendioate **I** to the aldehyde carbonyl group of the phenylglyoxal would yield iminium–oxoanion intermediate **II**, which can be tautomerized to intermediate **III**. γ -Lactonization of intermediate **III** would produce the 5-oxo-2,5-dihydro-3-furancarboxylates.

CONCLUSIONS

In conclusion, we have developed a simple way for the synthesis of furans using HPA-ZSM-5 as an efficient catalyst at room temperature in dichloromethane. The zeolite catalyst has been characterized by XRD, FE-SEM, EDS, FT-IR, and N2-adsorption analysis. The structures of the products were deduced from their 1H NMR, 13C NMR, FT-IR, and elemental analyses. The advantages of this method include its simplicity, the reusability of the catalyst, low catalyst loading, and easy separation of products.

CONFLICTS OF INTEREST

The authors declare that there are no conflicts of interest regarding the publication of this paper.

REFERENCES

[1] Kumar N, Gusain A, Kumar J, Singh R, Hota PK. Anti-oxidation properties of 2-substituted furan derivatives: A mechanistic study. Journal of Luminescence. 2021;230:117725.

[2] Karipcin F, Atis M, Sariboga B, Celik H, Tas M. Structural, spectral, optical and antimicrobial properties of synthesized 1-benzoyl-3-furan-2-ylmethyl-thiourea. Journal of Molecular Structure. 2013;1048:69-77.

[3] Akolkar HN, Dengale SG, Deshmukh KK, Karale BK, Darekar NR, Khedkar VM, et al. Design, Synthesis and Biological Evaluation of Novel Furan & Thiophene Containing Pyrazolyl Pyrazolines as Antimalarial Agents. Polycyclic Aromatic Compounds. 2020:1-13.

[4] Kassem AF, Nassar IF, Abdel-Aal MT, Awad HM, El-Sayed WA. Synthesis and Anticancer Activity of New ((Furan-2-yl)-1,3,4-thiadiazolyl)-1,3,4-oxadiazole Acyclic Sugar Derivatives. Chemical and Pharmaceutical Bulletin. 2019;67(8):888-95.

[5] Katritzky AR, Tala SR, Lu H, Vakulenko AV, Chen Q-Y, Sivapackiam J, et al. Design, Synthesis, and Structure–Activity Relationship of a Novel Series of 2-Aryl 5-(4-Oxo-3-phenethyl-2-thioxothiazolidinylidenemethyl)furans as HIV-1 Entry Inhibitors. Journal of Medicinal Chemistry. 2009;52(23):7631-9.

[6] Zeni G, Lüdtke DS, Nogueira CW, Panatieri RB, Braga AL, Silveira CC, et al. New acetylenic furan derivatives: synthesis and anti-inflammatory activity. Tetrahedron Letters. 2001;42(51):8927-30.

[7] Sheela A, Vijayaraghavan R. Synthesis, spectral characterization, and antidiabetic study of new furan-based vanadium(IV) complexes. Journal of Coordination Chemistry. 2011;64(3):511-24.

[8] Tufail F, Saquib M, Mishra A, Tiwari J, Verma SP, Dixit P, et al. Potash Alum as a Sustainable Heterogeneous Catalyst: A One-Pot Efficient Synthesis of Highly Functionalized Pyrrol-2-ones and Furan-2-ones. Polycyclic Aromatic Compounds. 2020:1-11.

[9] Salahi S, Maghsoodlou MT, Hazeri N, Movahedifar F, Doostmohammadi R, Lashkari M. Acidic ionic liquid N-methyl 2-pyrrolidonium hydrogen sulfate as an efficient catalyst for the one-pot multicomponent preparation of 3,4,5-substituted furan-2(5H)-ones. Research on Chemical Intermediates. 2015;41(9):6477-83.

[10] Shahraki M, Habibi-Khorassani SM, Dehdab M. Effect of different substituents on the one-pot formation of 3,4,5-substituted furan-2(5H)-ones: a kinetics and mechanism study. RSC Advances. 2015;5(65):52508-15.

[11] Nagarapu L, Kumar UN, Upendra P, Bantu R. Simple, Convenient Method for the Synthesis of Substituted Furan-2(5H)-one Derivatives Using Tin(II) Chloride. Synthetic Communications. 2012;42(14):2139-48.

[12] Narayana Murthy S, Madhav B, Vijay Kumar A, Rama Rao K, Nageswar YVD. Facile and efficient synthesis of 3,4,5-substituted furan-2(5H)-ones by using β-cyclodextrin as reusable catalyst. Tetrahedron. 2009;65(27):5251-6.

[13] Doostmohammadi R, Maghsoodlou MT, Hazeri N, Habibi-Khorassani SM. An efficient one-pot multi-component synthesis of 3,4,5-substituted furan-2(5H)-ones catalyzed by tetra-n-butylammonium bisulfate. Chinese Chemical Letters. 2013;24(10):901-3.

[14] Shafiee MRM, Mansoor SS, Ghashang M, Fazlinia A. Preparation of 3,4,5-substituted furan-2(5H)-ones using aluminum hydrogen sulfate as an efficient catalyst. Comptes Rendus Chimie. 2014;17(2):131-4.

[15] Bahramian F, Fazlinia A, Mansoor SS, Ghashang M, Azimi F, Najafi Biregan M. Preparation of 3,4,5-substituted furan-2(5H)-ones using HY Zeolite nano-powder as an efficient catalyst. Research on Chemical Intermediates. 2016;42(8):6501-10.

[16] Kangani M, Maghsoodlou M-T, Hazeri N. Vitamin B_{12}: An efficient type catalyst for the one-pot synthesis of 3,4,5-trisubstituted furan-2(5H)-ones and N-aryl-3-aminodihydropyrrol-2-one-4-carboxylates. Chinese Chemical Letters. 2016;27(1):66-70.

[17] Shahbazi-Alavi H, Safaei-Ghomi J, Dehghan MS. Ionic liquid-tethered colloidal silica nanoparticles as a reusable and effective catalyst for the synthesis of phenazines. Nanochemistry Research. 2020;5(2):111-9.

[18] Shahbazi-Alavi H, Safaei-Ghomi J. Synthesis of pyrimidines using nano-$NiZr_4(PO_4)_6$ as a retrievable and robust heterogeneous catalyst. Nanochemistry Research. 2020;5(2):141-7.

[19] Timofeeva MN. Acid catalysis by heteropoly acids. Applied Catalysis A: General. 2003;256(1):19-35.

[20] Sofia LTA, Krishnan A, Sankar M, Kala Raj NK, Manikandan P, Rajamohanan PR, et al. Immobilization of Phosphotungstic Acid (PTA) on Imidazole Functionalized Silica: Evidence for the Nature of PTA Binding by Solid State NMR and Reaction Studies. The Journal of Physical Chemistry C. 2009;113(50):21114-22.

[21] Molnár Á, Keresszegi C, Török B. Heteropoly acids

immobilized into a silica matrix: characterization and catalytic applications. Applied Catalysis A: General. 1999;189(2):217-24.
[22] Sunita G, Devassy BM, Vinu A, Sawant DP, Balasubramanian VV, Halligudi SB. Synthesis of biodiesel over zirconia-supported isopoly and heteropoly tungstate catalysts. Catalysis Communications. 2008;9(5):696-702.
[23] Waghmare NG, Kasinathan P, Amrute A, Lucas N, Halligudi SB. Titania supported silicotungstic acid: An efficient solid acid catalyst for veratrole acylation. Catalysis Communications. 2008;9(10):2026-9.
[24] Izumi Y, Hisano K, Hida T. Acid catalysis of silica-included heteropolyacid in polar reaction media. Applied Catalysis A: General. 1999;181(2):277-82.
[25] Safaei-Ghomi J, Kareem Abbas A, Shahpiri M. Synthesis of imidazoles promoted by $H_3PW_{12}O_{40}$-amino-functionalized $CdFe_{12}O_{19}@SiO_2$ nanocomposite. Nanocomposites. 2020;6(4):149-57.
[26] Mukai SR, Shimoda M, Lin L, Tamon H, Masuda T. Improvement of the preparation method of "ship-in-the-bottle" type 12-molybdophosphoric acid encaged Y-type zeolite catalysts. Applied Catalysis A: General. 2003;256(1):107-13.
[27] Wang J, Zhu H-O. Alkylation of 1-Dodecene with Benzene over $H_3PW_{12}O_{40}$ Supported on Mesoporous Silica SBA-15. Catalysis Letters. 2004;93(3):209-12.
[28] Bordoloi A, Lefebvre F, Halligudi SB. Selective oxidation of anthracene using inorganic–organic hybrid materials based on molybdovanadophosphoric acids. Journal of Catalysis. 2007;247(2):166-75.
[29] Liu P, Zhang Z, Jia M, Gao X, Yu J. ZSM-5 zeolites with different SiO_2/Al_2O_3 ratios as fluid catalytic cracking catalyst additives for residue cracking. Chinese Journal of Catalysis. 2015;36(6):806-12.
[30] Xue Z, Ma J, Zhang T, Miao H, Li R. Synthesis of nanosized ZSM-5 zeolite with intracrystalline mesopores. Materials Letters. 2012;68:1-3.
[31] Bhamare VS, Kulkarni RM, Santhakumari B. 5% Barium doped zinc oxide semiconductor nanoparticles for the photocatalytic degradation of Linezolid: synthesis and characterisation. SN Applied Sciences. 2018;1(1):103.
[32] Bhamare VS, Kulkarni RM. Photocatalytic degradation of pharmaceutical drug zidovudine by undoped and 5 % barium doped zinc oxide nanoparticles during water treatment: Synthesis and characterisation. International Journal of Applied Pharmaceutics. 2019;11(1):227.
[33] Bhamare VS. Mechanistic insight into photocatalytic degradation of antibiotic cefadroxil by 5 % barium/zinc oxide nanocomposite during water treatment. Emergent Materials. 2021.
[34] Bhamare VS, Kulkarni RM. Synthesis, characterisation and photocatalytic degradation of linezolid during water treatment by ruthenium doped titanium dioxide semiconducting nanoparticles. AIP Conference Proceedings. 2019;2142(1):210005.
[35] Bhamare VS, Kulkarni RM. Photocatalytic degradation of zidovudine by 0.8% ruthenium doped titanium dioxide nanoparticles during water treatment: synthesis, characterisation, kinetics and mechanism. Desalination and water treatment. 2020;182:288-98.
[36] Javidi J, Esmaeilpour M, Rahiminezhad Z, Dodeji FN. Synthesis and Characterization of $H_3PW_{12}O_{40}$ and $H_3PMo_{12}O_{40}$ Nanoparticles by a Simple Method. Journal of Cluster Science. 2014;25(6):1511-24.